Polymer Chemistry

Accepted Manuscript

ROYAL SOCIETY OF CHEMISTRY

www.rsc.org/polymers

Polymer Chemistry

RSCPublishing

ARTICLE

Thermoresponsive Properties of 3-, 4-, 6-, and 12-Armed Star-Shaped Poly[2-(dimethylamino)ethyl methacrylate]s Prepared by Core-First Group Transfer Polymerization

Cite this: DOI: 10.1039/x0xx00000x

Received 00th January 2012,
Accepted 00th January 2012

DOI: 10.1039/x0xx00000x

www.rsc.org/

Seiya Kikuchi,[a] Yougen Chen,[b] Keita Fuchise,[b] Kenji Takada,[a] Junsuke Kitakado,[a] Shin-ichiro Sato,[b] Toshifumi Satoh,[b] and Toyoji Kakuchi*[b]

The *t*-Bu-P_4-catalyzed group transfer polymerization (GTP) of 2-(dimethylamino)ethyl methacrylate (DMAEMA) using multi-functional GTP initiators that bear multiple silyl ketene acetal moieties (MTS_3, MTS_4, MTS_6, and MTS_{12}) homogenously proceeded and rapidly completed to afford well-defined star-shaped poly[2-(dimethylamino)ethyl methacrylate]s (*s*-PDMAEMAs) with relatively narrow polydispersities. The molecular weights (M.W.s) of the *s*-PDMAEMAs were well-controlled by optimizing the molar ratios of the monomer to initiators. For the structural analyses, the arm number and length uniformity of each *s*-PDMAEMA were then investigated by arm cleavage experiments using a transesterification method. The thermoresponsive properties in an aqueous solution of the resulting *s*-PDMAEMAs together with their analogous linear PDMAEMAs (*l*-PDMAEMAs), in terms of polymer concentration, molecular weight, and arm number, were eventually elucidated based on turbidimetry curves.

Introduction

Thermoresponsive polymers, exhibiting a reversible temperature-induced phase transition and phase separation around a critical temperature referred to as the cloud point (T_c), have attracted much attention due to their wide potential applications for numerous purposes, such as bioconjugates, sensing materials, and vectors in drug delivery systems.[1-3] These applications are based on the abrupt changes in aqueous solubility of a polymer at either an upper critical solution temperature (UCST) upon cooling or a lower critical solution temperature (LCST) upon heating. According to the recently advertised applications, such polymers have also been addressed as ″smart polymers″. Since the discovery of the thermal phase transition phenomenon of poly(*N*-isopropylacrylamide) (PNIPAM) in the mid-1960s,[4] many types of thermoresponsive polymers have been synthesized. Among them, the UCST-type polymers are relatively less reported, including the well-studied poly(ethylene oxide), poly(vinyl methyl ether), alkyl-modified poly(vinyl alcohol), poly(hydroxyethylmethacrylate), polybetaines, poly(acrylic acid) and the like.[5] In comparison, most thermoresponsive polymers belong to the LCST-type class, including many types of polymers such as some of poly(*N*-alkyl (meth)acrylamide)s, poly(*N*-vinylalkylamide)s, poly(meth)acrylates, polyphosphoesters, poly(vinyl ether)s, polyethers, and poly(alkyloxide)s.[6] For the LCST-type polymers, it has been widely accepted that they, at low temperature, homogeneously dissolve in water in the form of a hydrated random-coil structure. On the other hand, the coil chains start to dehydrate along the polymer chain upon heating their aqueous solutions above the T_c, enabling the polymer chains themselves to transform from a coil state to a globule state (phase transition). Immediately after the phase transition, the polymer globules aggregate to form polymer-rich and water-rich domains due to the hydrophobic interactions, therefore, inducing a phase separation.[7] In the past decades, many research groups have revealed that the thermal phase transition and separation of a thermoresponsive polymer is significantly dependent not only on its intrinsic architectural nature, *e.g.*, chain length, end group, and block composition, but also on external stimulus like pH and ionic strength.[8-10] In order to clarify the relationship between the thermoresponsive property and a specific variable which could be a functional end group or an external stimuli, many researchers have made substantial contributions in such aspects. For instance,

PNIPAM, one of the most representative thermoresponsive polyacrylamides, conventionally shows a T_c around 32 °C,[11] nevertheless, it has a tunable T_c from 34.8 °C to 44.6 °C by introducing various terminal groups.[12, 13] Poly[oligo(ethylene glycol) methacrylate]s are another type of LCST-type thermoresponsive polymers, of which T_c can be precisely adjusted in a range of 9-90 °C by changing the degree of polymerization (DP) of oligo(ethylene glycol) in the side chain and the comonomer composition of different types of oligo(ethylene glycol) methacrylates.[7, 14-16] As another example, poly[2-(dimethylamino)ethyl methacrylate] (PDMAEMA), one of the most representative thermoresponsive polymethacrylates, usually displays a T_c around 40 °C, while its T_c is changeable in the range of 32.2-46.6 °C by varying its molecular weight,[17] and in the range of 25.0 ~ 78.0 °C by adjusting the pH of its aqueous solution within 7.0 ~ 10.0.[18] Thereafter, many researchers also devoted their efforts in elucidating the topological effect of a branched thermoresponsive polymer, such as those with a star, comb, or dendritic architecture, on its thermoresponsive property because these specially structured polymers behave rather differently in comparison to their linear analogues. For instance, Xu and Liu et al. reported that star and brush PNIPAM with compact arms exhibited a two temperature-induced phase transitions. For details, see a recent review article in the literatures.[7] Among the branched topologies, a star polymer, having a relatively simple structure, seems to be an ideal candidate for this purpose. Actually, some research groups have engaged in this research area. As some representative examples, Whittaker et al. investigated the thermoresponsive behavior of a four-armed star-shaped PNIPAM obtained from a reversible addition-fragmentation chain transfer (RAFT) polymerization based on the core-first method.[19] Liu et al. reported seven- and twenty-one-armed PNIPAMs synthesized by the atom transfer radical polymerization (ATRP) using cyclodextrin-derived initiators.[20] Müller et al. reported the thermoresponsive properties of the star-shaped PDMAEMA (*s*-PDMAEMA) synthesized by both RAFT polymerization and ATRP methods based on a core-first strategy though the initiating efficiency in their studies was very low.[18, 21, 22] Surprisingly, the studies in this field are limited to a few reports, and a theoretical approach, in particular, is less revealed. Thus, it is of great meaning to provide a much deeper insight into this aspect.

A unique feature of a star-shaped polymer is that it has a densely packed core and a less-compact outer shell. This nature might make a star-shaped polymer be an interesting object when it is a thermoresponsive polymer. For the synthesis of the above mentioned star-shaped thermoresponsive polyacrylamides and poly(meth)acrylates, the controlled radical polymerizations (CRPs) have been the most employed based on either a core-first or an arm-first method.[23] The core-first CRPs are easily done and can render the resulting star-shaped polymers with moderate control over the molecular weight and molecular weight distribution. However, the CRPs based on the core-first strategy can hardly avoid inter- and intramolecular radical recombinations especially when the arm density in a star polymer and/or the monomer conversion is high. Such radical recombinations would result in a severe heterogeneity of the arm length. In contrast, the arm-first CRPs can afford homogeneous arms but involve a coupling reaction between the pre-prepared arms and a linker. With an extremely cautious operation, the coupling reaction can be perfectly achieved. However, it is difficult to assure complete coupling of the pre-prepared arms to a certain linker due to the steric hindrance at the core especially when the linker has dense coupling sites. Ionic polymerization methods have also been used to synthesize some of the branched thermoresponsive polymers, which basically involved extremely strict polymerization conditions such as super-high vacuum and had a limitation in usable monomers.[24] Based on this background, we herein focus our attention on the group transfer polymerization (GTP), which is considered to be a recombination-free polymerization with neutral propagating ends living during the polymerization process. In our previous reports, the precise synthesis of star-shaped poly(methyl methacrylate)s (PMMA) has been readily achieved by the core-first GTP using either a base or an acid catalyst, in which the arm uniformity and arm number up to six were experimentally proven.[25, 26] Thus, it is rational to expect that the GTP method can also be used to synthesize well-defined star-shaped thermoresponsive polymethacrylates. This study describes: (1) the precise synthesis of *s*-PDMAEMAs by core-first GTP using various multi-functional GTP initiators, as shown in Scheme 1, (2) evaluation of the arm uniformity of the *s*-PDMAEMAs, and (3) the thermoresponsive behaviors of the *s*-PDMAEMAs in terms of polymer concentration, molecular weight, and arm number. The results of this study are expected to provide more fundamental understanding in regard to the thermal transition behavior of star-shaped thermoresponsive polymers.

Scheme 1. The *t*-Bu-P_4-catalyzed group transfer polymerization of 2-(dimethylamino)ethyl methacrylate (DMAEMA) using multi-functional initiators (MTS_m).

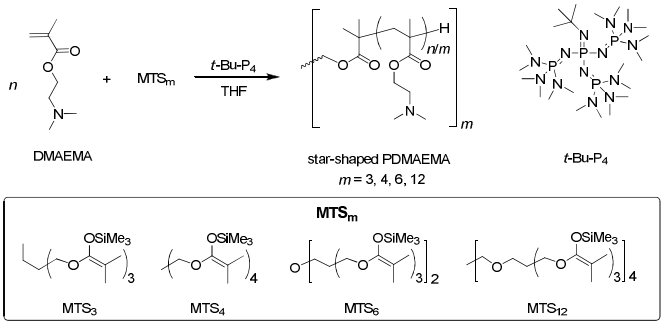

Experimental

Materials. 2-(Dimethylamino)ethyl methacrylate (DMAEMA) and (2-dimethylamino)ethanol were purchased from Tokyo Kasei Kogyo Co., Ltd., (TCI) and used after distillation over CaH_2 under reduced pressure. 1-*tert*-Butyl-4,4,4-tris (dimethylamino)-2,2-bis[tris(dimethylamino)-phosphoranylidenamino]-2Λ^5,4Λ^5-catenadi(phosphazene) (*t*-Bu-P_4, 1.0 mol L^{-1} in *n*-hexane) was commercially available from Sigma-Aldrich Chemicals Co. and used as received. Sodium hydride (60%, dispersion in paraffin liquid), diisopropyl azodicarboxylate (DIAD), triphenylphosphine

(PPh_3), and benzoic acid were purchased from TCI and used as received. 1-Methoxy-1-trimethylsiloxy-2-methyl-1-propene (MTS) was purchased from TCI and used after distillation under reduced pressure without any drying agent. The star-shaped initiators, 1,1,1-tris[2-methyl-1-(trimethylsilyloxy)prop-1-enyloxy]propane (MTS_3), tetrakis{[2-methyl-1-(trimethylsilyloxy)prop-1-enyloxy]methyl}methane (MTS_4), and bis{2,2,2-tris[2-methyl-1-(trimethylsilyloxy)prop-1-enyloxy]ethyl}ether (MTS_6) were used as reported in our previous study.[25] Tetrahydrofuran (THF, > 99.5 %, dehydrated stabilizer free) was purchased from Kanto Chemical Co., Inc., and distilled over Na/benzophenone in an argon atmosphere prior to use. All other reagents were used as received without further purification.

Instruments. The ^{1}H and ^{13}C NMR spectra were recorded by JEOL JNM-A400II and JEOL-ECP-400 instruments. All polymerizations were carried out in an MBRAUN stainless steel glove box equipped with a gas purification system (molecular sieves and copper catalyst) and a dry argon atmosphere (H_2O, O_2 < 1 ppm). The moisture and oxygen contents in the glove box were monitored by an MB-MO-SE 1 and an MB-OX-SE 1, respectively. The number-average molecular weights ($M_{n,SEC}$s) and molecular weight distributions (M_w/M_ns) of the polymers were measured by size exclusion chromatography (SEC) at 40 °C using a Jasco high performance liquid chromatography (HPLC) system (PU-980 Intelligent HPLC pump, CO-965 Column oven, RI-930 Intelligent RI detector, and Shodex DEGAS KT-16) equipped with a Shodex Asahipak GF-310 HQ column (linear, 7.6 mm × 300 mm; pore size, 20 nm; bead size, 5 μm; exclusion limit, 4×10^4) and a Shodex Asahipak GF-7M HQ column (linear, 7.6 mm × 300 mm; pore size, 20 nm; bead size, 9 μm; exclusion limit, 4×10^7) in DMF containing 0.01 mol L^{-1} lithium chloride (LiCl) at the flow rate of 0.4 mL min^{-1}, and calculated on the basis of a poly(*N*,*N*-dimethylacrylamide) calibration. The absolute molecular weight ($M_{w,MALS}$) was estimated by SEC in DMF containing 0.01 mol L^{-1} LiCl (1.0 mL min^{-1}) at 40 °C using an Agilent 1100 series instrument equipped with two Shodex KF-804L columns (linear, 8.0 mm × 300 mm; exclusion limit, 4×10^5; bead size, 7 μm), a DAWN 8 multi-angle laser light scattering (MALS) detector (Wyatt Technology, Santa Barbara, CA), a Viscostar viscosity detector (Wyatt Technology), and an Optilab rEX refractive index detector (Wyatt Technology). The IR spectra were recorded using a Perkin-Elmer Paragon 1000 FT-IR instrument. The hydrodynamic diameters of the obtained polymer in deionized water were analyzed using a fiber dynamic light scattering spectrophotometer (FDLS-300, Otsuka Electronics Co.) equipped with a 532 nm laser at a 90° scattering angle, and zeta potential and particle size analyzer (Delsa nano HC, BECKMAN COULTER) equipped with a 658 nm laser at a 15° scattering angle. The cloud point measurements were performed on the ultraviolet-visible (UV-vis) spectrometer by passing through a 10-mm path-length cell using a Jasco V-550 spectrophotometer equipped with an EYELA NCB-1200 temperature controller.

Synthesis of linear and star-shaped PDMAEMAs. All the *l*- and *s*-PDMAEMAs were prepared by the same procedure. The preparation of a three-armed *s*-PDMAEMA under the condition of $[DMAEMA]_0/[MTS_3]_0/[t\text{-Bu-P}_4]_0$ = 120/1/0.05 was typically described as follows: a stock solution (83.3 μL) of MTS_3 (41.7 μmol, 0.50 mol L^{-1}) in THF and a stock solution (20.8 μL) of *t*-Bu-P_4 (0.208 μmol, 0.01 mol L^{-1}) in THF in a test tube were stirred for a few minutes, and then a stock solution (2.0 mL) of DMAEMA (5.0 mmol, 2.5 mol L^{-1}) in THF was added within about 10 min. The polymerization was quenched after 1 h by adding a small amount of methanol. A portion of the polymerization mixture was used for the determination of the DMAEMA conversion, which was directly estimated from the ^{1}H NMR measurement of the polymerization mixture. The crude product was purified by passing through a silica pad with THF. Conversion, >99 %; $M_{w,MALS}$, 19.3 kg mol^{-1}; *Đ*, 1.25; yield, 535 mg (68%).

Cleavage of six-armed *s*-PDMAEMA. 2-Dimethylaminoethanol (4.08 mL, 63.6 mmol) was slowly added to a suspension of NaH (1.52 g, 63.6 mmol) in dry THF (6.36 mL) at 0 °C. After 2 h of stirring, a six-arm *s*-PDMAEMA (run 13; $M_{w,MALS}$, 30.2 kg mol^{-1}; *Đ*, 1.20; 200 mg) in dry THF (2.5 mL) was added to the solution at ambient temperature. After 24 h of stirring, the solution was neutralized with 1N hydrochloric acid (12 mL). The crude product was purified by dialysis in a cellophane tube (Spectra/Por® 6 Membrane, MWCO: 1 000) against distilled water followed by lyophilization. The resulting partially hydrolyzed PDMAEMA arm polymer (132 mg, 84.2 μmol) was esterified with 2-dimethylaminoethanol (143 μL, 1.43 mmol), DIAD (281 μL, 1.43 mmol), and triphenylphosphine (389 mg, 1.43 mmol) in dry THF. The completion of the reaction was confirmed from the IR measurement. The crude product was purified by dialysis in a cellophane tube (Spectra/Por® 6 Membrane, MWCO: 1 000) against distilled water followed by lyophilization. Yield, 95.0 mg (48%).

Determination of Cloud Point (T_c). Typically, an aqueous solution of the polymer (2.0 g L^{-1}) was prepared and cooled in an ice bath for 2 min, and the resulting clear solution was then transferred to a 10-mm length poly(methyl methacrylate) cell. The transmittance of the aqueous solution at 500 nm was recorded by a UV-vis spectrophotometer equipped with a temperature controller. The solution was gradually heated at the heating rate of 1.0 °C min^{-1}.

Results and discussion

Synthesis of *s*-PDMAEMAs. For the core-first syntheses of the *s*-PDMAEMAs by GTP, multi-functional GTP initiators noted as MTS_3, MTS_4, and MTS_6 were used as before.[25] In order to further increase the arm number, we newly synthesized another initiator that bears twelve silyl enolate moieties, referred to as MTS_{12} (see ESI). The chemical structure information of MTS_{12} was verified by the ^{1}H and ^{13}C NMR measurements, as shown in Figure S1. For GTPs of DMAEMA, a phosphazene base, *t*-Bu-P_4, was used as the catalyst, and all polymerizations were carried out in THF under the conditions of 25 °C, argon atmosphere, and polymerization time = 1 h. As observed in our previous study, the ratio of $[t\text{-Bu-P}_4]_0$ to $[Initiator]_0$ ($[t\text{-Bu-P}_4]_0/[I]_0$) significantly affected the polymerization rate and molecular weight distribution and its value (*Đ*) of the resulting

polymer. Thus, the $[t\text{-Bu-P}_4]_0/[I]_0$ ratio was optimized corresponding to a certain polymerization. For a specified type of *s*-PDMAEMA, polymers with different molecular weights were synthesized by changing the initial $[DMAEMA]_0/[I]_0$ ratio. As shown in Table 1, the syntheses of three-, four-, six-, and twelve-armed *s*-PDMAEMAs (*s*-PDMAEMA$_3$s, *s*-PDMAEMA$_4$s, *s*-PDMAEMA$_6$s, and *s*-PDMAEMA$_{12}$s, respectively) were carried out with their $[DMAEMA]_0/[I]_0$ ratios ranging from 120 ~ 1200 (runs 5-8), 120 ~ 1200 (runs 9-12), 120 ~ 1200 (runs 13-16), and 120 ~ 2400 (runs 17-21), respectively. The SEC(RI) determinations shown in Figure S2 suggest that the molecular weight distributions of all the *s*-PDMAEMAs are monodisperse. From the SEC(MALS) measurements, their absolute molecular weights ($M_{w,MALS}$s) were determined in the ranges of 19.3 ~ 160, 24.0 ~ 254, 30.2 ~ 296, and 34.3 ~ 419 kg mol^{-1}, respectively. The number average molecular-weights ($M_{n,MALS\text{-}est.}$s) of the three-, four-, six-, and twelve-armed *s*-PDMAEMAs estimated by the equation of $M_{n,MALS\text{-}est.} = M_{w,MALS}/Đ$ were respectively in the ranges of 15.4 ~ 126, 19.7 ~ 192, 25.2 ~ 233, and 30.4 ~ 301 kg mol^{-1}, which approximately agreed with their theoretical number-average molecular weights ($M_{n,theo.}$s; 19.2 ~ 189, 19.2 ~ 189, 19.5 ~ 189, and 20.4 ~ 379 kg mol^{-1}, respectively; for details, see Table 1). For comparison, *l*-PDMAEMAs with the theoretical degrees of polymerization (DP) = 50 ~ 600 (runs 1-4) were also synthesized using MTS, and their $M_{w,MALS}$s are in the range of 11.8 ~ 105 kg mol^{-1}. It is worth noting that the synthesized *l*- and *s*-PDMAEMAs have *Đ*s in the range of 1.09 ~ 1.39. They are relatively broader than those of the previously reported star PMMAs though the applied polymerization conditions were almost the same. We assigned the relatively broader *Đ*s to the interference

Table 1. *t*-Bu-P$_4$-catalyzed GTPs of DMAEMA using various multi-functional initiators [a]

run	Initiator (I)	$[M]_0/[I]_0/[t\text{-Bu-P}_4]_0$	$M_{n,theo.}$ [d] (kg mol^{-1})	$M_{n,MALS\text{-}est.}$ [e] (kg mol^{-1})	$M_{w,MALS}$ [f] (kg mol^{-1})	*Đ* [g]
1[b]	MTS	50/1/0.010	7.9	10.2	11.8	1.16
2[c]		100/1/0.005	15.8	17.3	22.1	1.28
3[c]		200/1/0.005	31.5	40.3	47.5	1.18
4[c]		600/1/0.005	94.4	78.9	105	1.33
5[c]	MTS$_3$	120/1/0.005	19.2	15.4	19.3	1.25
6[c]		300/1/0.005	47.5	46.0	55.7	1.21
7[c]		600/1/0.005	94.7	88.3	106	1.20
8[b]		1200/1/0.020	189	126	160	1.27
9[c]	MTS$_4$	120/1/0.005	19.2	19.7	24.0	1.22
10[c]		400/1/0.005	63.3	75.0	87.0	1.16
11[c]		600/1/0.005	94.7	102	128	1.26
12[b]		1200/1/0.050	189	192	254	1.32
13[b]	MTS$_6$	120/1/0.005	19.5	25.2	30.2	1.20
14[c]		300/1/0.005	47.8	58.3	63.5	1.09
15[b]		600/1/0.050	95.0	102	131	1.29
16[b]		1200/1/0.050	189	233	296	1.27
17[b]	MTS$_{12}$	120/1/0.010	20.4	30.4	34.3	1.13
18[b]		240/1/0.010	39.3	50.5	61.6	1.22
19[b]		600/1/0.050	95.8	88.4	114	1.29
20[b]		1200/1/0.020	190	167	199	1.19
21[b]		2400/1/0.030	379	301	419	1.39

[a] Solvent, THF; temp., r.t.; conv., >99% determined by ^{1}H NMR in $CDCl_3$. [b] $[DMAEMA]_0$, 1.0 mol L^{-1}. [c] $[DMAEMA]_0$, 2.0 mol L^{-1}. [d] $M_{n,theo.} = ([DMAEMA]_0/[I]_0) \times conv. \times (M.W.\ of\ DMAEMA) + (M.W.\ of\ desilylated\ initiator)$. [e] $M_{n,MALS\text{-}est.} = M_{w,MALS}/Đ$. [f] Determined by SEC(MALS) in DMF containing 0.01 mol L^{-1} LiCl. [g] Determined by SEC(RI) in DMF containing 0.01 mol L^{-1} LiCl on the basis of poly(*N*,*N*-dimethylacrylamide) (PDMAA) standards.

Polymer Chemistry RSCPublishing

ARTICLE

toward the trimethylsilyl groups at the living polymer chain ends, which was caused by the tertiary amino groups either from the polymer chains themselves or monomers, as reported by Taton et al.[27] This interference is also somewhat considered to be the incentive for the deviation of the $M_{n,MALS\text{-}est.}$ from $M_{n,theo.}$.

Next, for a well-controlled star polymer, the arm number and length homogeneity need to be clarified. To achieve this attempt, the ester cleavage experiments of the core linkage were carried out under extremely basic conditions as described in the experimental section. The retro-esterifying cleavage was rather successful to afford the partially hydrolyzed (at monomer esters) *l*-PDMAEMA arms, which were eventually esterified back to the *l*-PDMAEMA arms. Figure S3 typically shows the SEC traces of both the parent *s*-PDMAEMA$_6$ (run 13; $M_{w,MALS}$, 30.2 kg mol^{-1}; $Đ$, 1.20) and its cleaved *l*-PDMAEMA arm. Obviously the SEC trace of the *l*-PDMAEMA arm significantly shifts to the lower molecular-weight region after the cleavage as compared to that of its parent *s*-PDMAEMA$_6$, while retaining a monomodal and narrow distribution ($Đ$ = 1.13). Moreover, MALDI-TOF MS measurements were also carried out to confirm the chemical structure of the cleaved *l*-PDMAEMA arm, from which two series of peaks together with a peak top around 3.5 kDa were observed in the spectra shown in Figure S4. Both series showed an equal peak distance of 157.21 Da which corresponds to the M.W. of the DMAEMA unit. In both peak series, the values of the sub-series (Δ) and main series (○) were in agreement with the M.W.s of the *l*-PDMAEMA arm cationized by a Na^+ and H^+, respectively. On the other hand, by roughly comparing the M_ns between the cleaved *l*-PDMAEMA (M_n = 3.5 kDa around peak top by MALDI-TOF MS) and its parent *s*-PDMAEMA$_6$ ($M_{n,theo.}$ = 19.5 kDa), the arm number calculated by $M_{n,theo.}$(*s*-PDMAEMA$_6$)/M_n(*l*-PDMAEMA) is 5.6. This value is rather close to the designed arm number of 6. The previously discussed analyses lead us to draw the conclusion that no side reactions (*e.g.*, back-biting reaction) occurred during the GTP of DMAEMA and the *s*-PDMAEMAs obtained from the core-first *t*-Bu-P$_4$-catalyzed GTPs have the desired arm number, uniform arm length and chemical composition.

Thermoresponsive properties of *s*-PDMAEMAs. The cloud point (T_c) in this study is defined as the temperature at which an extremum of the first derivation locates by differentiating the transmittance-vs-temperature curve (see Figure S5). Notably, the used term, T_c, is more likely to be a phase transition temperature when the transmittance of a polymer solution only changed slightly on a transmittance vs temperature curve. T_cs were also estimated by DLS measurements (for some typical examples, see Figure S6), which were very close to the values estimated by transmittance determinations using a UV-vis spectrophotometer. Thus, T_cs estimated from the UV-vis spectrophotometer were used in this study. First, the T_c dependence of each *s*-PDMAEMA of the respective polymer mass concentration in aqueous solution (C) was investigated, as shown in Figure 1. For the T_c measurements, *s*-PDMAEMA$_3$ (run 8; $M_{w,MALS}$, 160 kg mol^{-1}; $Đ$, 1.27), *s*-PDMAEMA$_4$ (run 12; $M_{w,MALS}$, 254 kg mol^{-1}; $Đ$, 1.32), *s*-PDMAEMA$_6$ (run 16; $M_{w,MALS}$, 296 kg mol^{-1}; $Đ$, 1.27), and *s*-PDMAEMA$_{12}$ (run 21; $M_{w,MALS}$, 419 kg mol^{-1}; $Đ$, 1.39) were used, and their Cs were varied in the range of 2.0 ~ 20 g L^{-1}. It was observed that the T_c decreased with increasing C of a specified polymer. Additionally, the optical transmittance showed a sharp decrease (fast responsive rate) for all the used *s*-PDMAEMAs when a high C like 20 g L^{-1} was employed, while its decrease gradually got slow and almost vanished (slow responsive rate) after decreasing the C to 2.0 g L^{-1}, even though the used *s*-PDMAEMAs had molecular weights higher than 100 kg mol^{-1}. The higher the C, the lower T_c a specified *s*-PDMAEMA exhibited and the faster thermoresponsive transition was observed in its transmittance curve. This can be reasonably explained by the enhanced entanglement among the polymer chains and the shortened diffusion time to get polymers aggregated largely because the inter-polymer distance decreases with the increasing C. For a detailed explanation, refer to reports in the literatures.[28, 29] Sequentially, the T_c-$M_{w,MALS}$ dependence of each type polymer was investigated at a fixed mass concentration of 2.0 g L^{-1} since the $M_{w,MALS}$ is usually a key issue affecting the T_c (Figure 2 a-f). It was found that the T_c of *l*-PDMAEMA or each *s*-PDMAEMA with its $M_{w,MALS}$ lower than a certain value (ca. 100 kg mol^{-1}) decreased with the increasing $M_{w,MALS}$, but conversely increased when the polymer has a $M_{w,MALS}$ higher than this value. For instance, the T_c of *s*-PDMAEMA$_3$ continuously declined from 41.0 to 36.5 °C with increasing $M_{w,MALS}$ in the range of 19.3 ~ 106 kg mol^{-1}, but adversely enhanced to 40.1 °C when the $M_{w,MALS}$ was 160 kg mol^{-1}. A similar thermoresponsive behavior was also observed for *l*-PDMAEMA and the other type of *s*-PDMAEMAs. We thus can exclude the possibility that the observed T_c trend is due to experimental error. The T_c dependence of $M_{w,MALS}$ in this case is quite distinct from those reported in other reports. For example, Whittaker et al. and Liu et al. separately reported that the T_c of the star-shaped PNIPAMs ($M_{w,MALS}$s < 70 kg mol^{-1}) showed an increasing tendency with increasing $M_{w,MALS}$.[19, 20] Pan et al. reported that the T_c of PNIPAM seemed not dependent on its molar mass and architecture.[30] In addition, Müller et al. and Patrickios et al. revealed that the T_c of *s*-PDMAEMAs with a gelatinized core exhibited a

decreasing tendency with increasing molar mass.[22, 31] The molar mass effect on the T_c is still not very clear. It is well known that the T_c dependence on $M_{w,MALS}$ can be readily affected by the polymer composition, end group, polymer concentration, etc. For a star polymer, the hydrophilicity/hydrophobicity of the core should also be considered. The phenomena observed in this study can be roughly explained by a "cooperative hydration" model advocated by Tanaka et al.[32] or somewhat by a diffusion determination model developed by Kitamura et al.[28, 29] Both of them have been used to interpret the phase separation behavior of PNIPAM.

The "cooperative hydration" model proposes that the collapse of the cooperative interaction between the water molecules that mutually hydrogen bond onto a polymer chain leads to a phase transition and separation behavior. In this model, it is considered that water molecules interact with hydrogen-bonding acceptors like carbonyl groups on a polymer chain in an aqueous solution, activate their protons to form hydrogen bonds, and further form clusters among themselves to stabilize its solution state. Based on this model, we describe our case in Figure 3. It is rational to assume that water molecules can randomly bond onto a polymer chain irrespective of the polymer shape, but the bonding degree significantly correlates with this factor. For a star polymer, the polymer-water hydrogen bonding interaction in the core regime can be considered to be much weaker (less hydrogen bonding network) as compared to a freely stretched *l*-PDMAEMA (many hydrogen bonding network) due to its compact effect caused by the high polymer chain density.

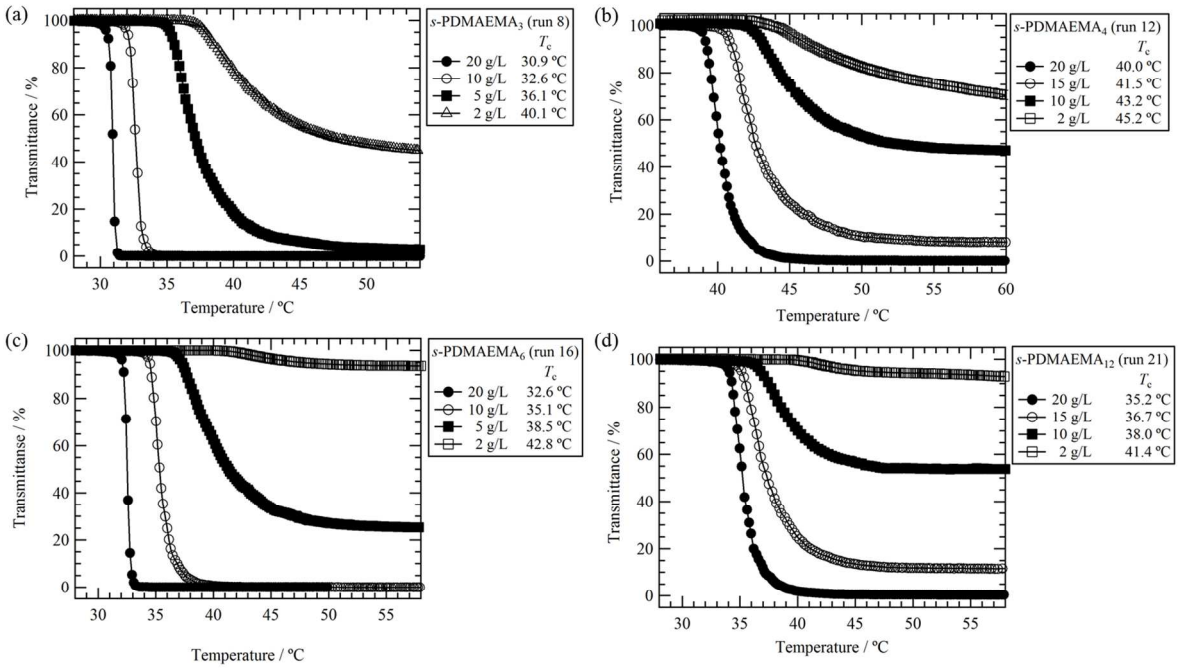

Figure 1. T_c dependence of respective *s*-PDMAEMA on mass concentration: (a) *s*-PDMAEMA$_3$ (run 8; $M_{w,MALS}$, 160 kg mol^{-1}), (b) *s*-PDMAEMA$_4$ (run 12; $M_{w,MALS}$, 254 kg mol^{-1}), (c) *s*-PDMAEMA$_6$ (run 16; $M_{w,MALS}$, 296 kg mol^{-1}), and (d) *s*-PDMAEMA$_{12}$ (run 21; $M_{w,MALS}$, 419 kg mol^{-1}).

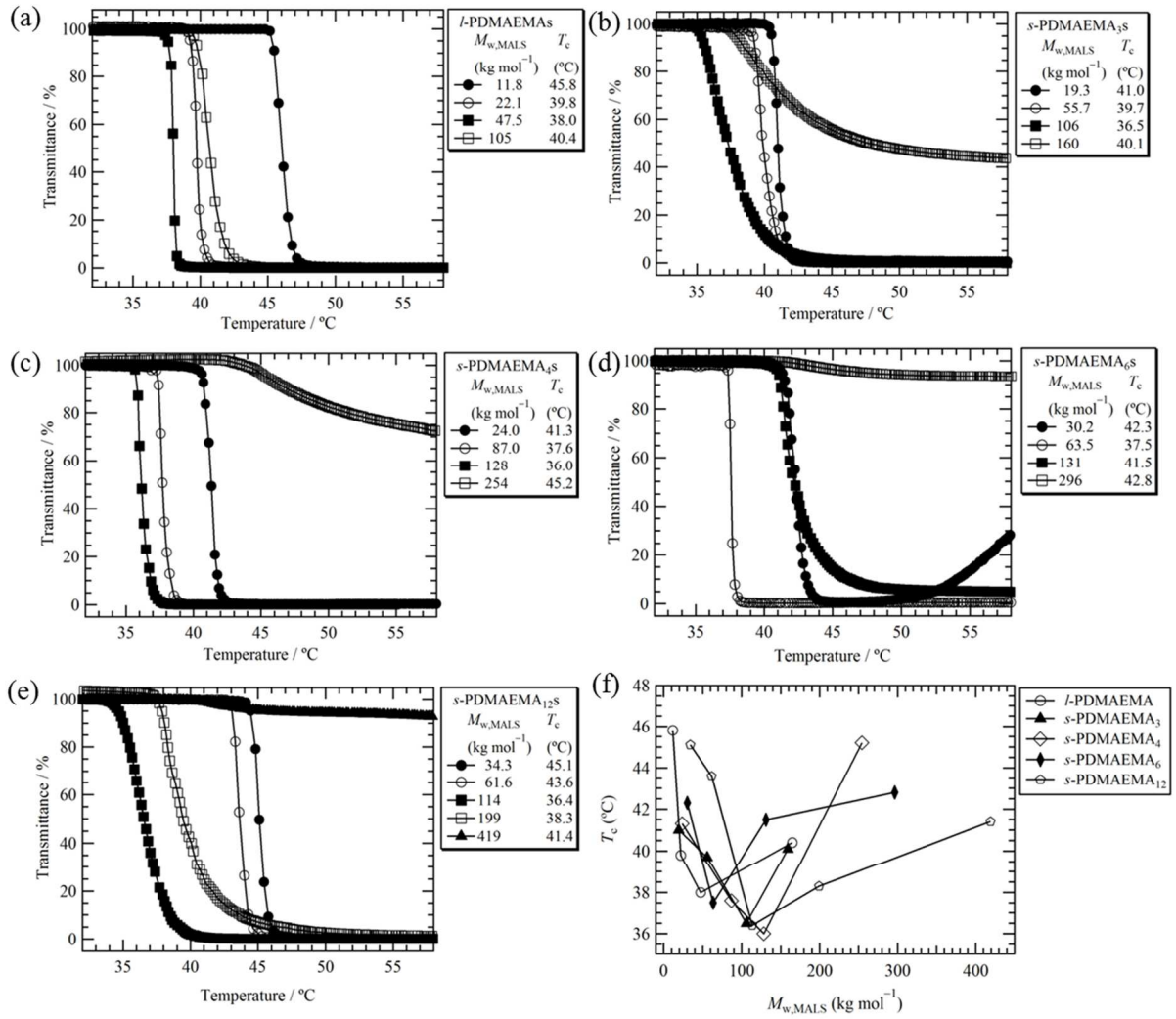

Figure 2. Optical transmittance dependence of *l*-PDMAEMA and respective *s*-PDMAEMA on molecular weight at a fixed mass concentration of 2.0 g L^{-1}: (a) *l*-PDMAEMA, (b) *s*-PDMAEMA$_3$, (c) *s*-PDMAEMA$_4$, (d) *s*-PDMAEMA$_6$, (e) *s*-PDMAEMA$_{12}$, and (f) an overall summary.

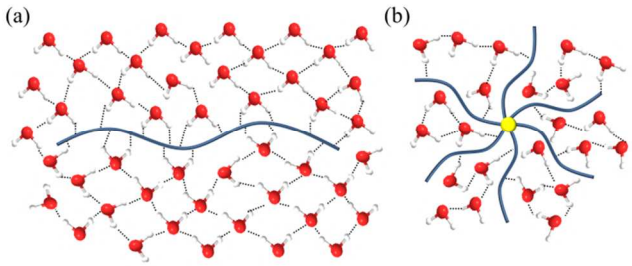

Figure 3. A proposed "cooperative hydration" model for a thermoresponsive polymer in an aqueous solution; (a) many hydrogen bonding networks in a linear polymer and (b) fewer hydrogen bonding networks in a star-shaped polymer.

However, this effect will significantly get weak at the outer parts of the arms. In other words, the water molecules poorly hydrogen bond onto polymer chains in the core region, but easily bond at the outer space of a star polymer, which causes a stepwise dehydration.[33, 34] Based on this assumption, the phenomena observed in our study can be in principle explained as the arm compact effect in a *s*-PDMAEMA ($M_{w,MALS}$ < ca.100 kg mol^{-1}) plays a dominant role so that the dehydration easily occurs along the whole polymer, which causes the formation of a hydrophobic globule and the consequent phase separation. In this $M_{w,MALS}$ region, the T_c dependence on $M_{w,MALS}$ can be explained by the modified Flory-Huggins theory.[35] On the contrary, the phase separation behavior changes when a *s*-PDMAEMA has an $M_{w,MALS}$ > 100 kg mol^{-1}. The dehydration occurring in this case is considered to be a stepwise process. That is, upon heating the polymer solution, the dehydration initially takes place in the core area and then along the polymer chains to the outer arms. During the dehydration at an early stage, a hydrophobic domain at the core can easily form, however, the outer chains are still hydrophilic. The *s*-PDMAEMA in this stage is prone to stabilize itself in solution and can thus hardly form big micelles or aggregates. Further heating (higher T_c) is needed to dehydrate the hydrated outer chains in order to further undergo an inter-polymer assembly (phase

separation). On the other hand, Kitamura et al. proposed a diffusion-controlled aggregation model to explain the M_n effect on the phase separation rate (thermoresponsive rate).[28, 29] In their observations, PNIPAMs had an optimum size for a quick thermoresponsive phase separation, and either a low or a high molecular weight showed a slower thermoresponsivity. For a high molecular weight polymer, the reason for its slow responsive rate was interpreted by them as follows: the globular size and solution viscosity correspondingly increase with the increasing molecular weight, resulting in slow diffusion of the globules and thus a slow responsive rate; the diffusion of globules becomes the determining factor when the polymer has a high molecular weight. This model can be readily used to explain the slow decrease in the optical transmittance of the PDMAEMAs with high molecular weight. The slow diffusion of globules interrupts their assembly and phase separation. Therefore, a high temperature is needed to induce the phase separation. The elucidation by these two models is also strongly supported by the investigation of the T_c-$M_{w,MALS}$ dependence of *s*-PDMAEMA$_{12}$ (run 21; $M_{w,MALS}$ = 419 kg mol^{-1}; $Đ$, 1.39) under the condition of a fixed molar concentration, as shown in Figure 4. It is well known that the T_c of a LCST-type thermoresponsive polymer usually exhibits a decreasing tendency when its molecular weight increases.[36] This trend was clearly observed for *s*-PDMAEMA$_{12}$ in the $M_{w,MALS}$ range of 34.3 ~ 199 kg mol^{-1}. However, the T_c reversed to the high value of 37.1 °C when *s*-PDMAEMA$_{12}$ has a $M_{w,MALS}$ of 419 kg mol^{-1}. The T_c reversal at the high $M_{w,MALS}$ is most likely due to the difficulty in forming micelles or big aggregates after the phase transition. The average hydrodynamic diameter (D_h) data of *s*-PDMAEMA$_{12}$ in Table 2 provide direct evidence for the above explanation. It was found that the D_h values after phase transition kept roughly constant values (Figure S6). Therefore, DLS measurements after phase transition were carried out only at 25 °C and 55 °C. With the increase in $M_{w,MALS}$, the D_h of *s*-PDMAEMA$_{12}$ in an aqueous solution at the high temperature of 55 °C showed a decreasing tendency. It is rather obvious that *s*-PDMAEMA$_{12}$ with a high $M_{w,MALS}$ is difficult to get itself aggregated largely though the solution temperature is high enough to induce phase transition.

Finally, we tried to elucidate the branching effect of *s*-PDMAEMAs on the T_c. Different types of *s*-PDMAEMAs with the same theoretical DP were used to ensure that all the used polymers have similar molecular weights. The T_cs of the *s*-PDMAEMAs with a low DP of 120 showed a regular increase with the increasing arm number of the *s*-PDMAEMA, as shown in Figure 5. Given that they have the same DP, this tendency is much likely to be attributed to the shortened arm length when the arm number increases and indicates that the entire molecular weight is seemingly not a key factor. On the other hand, the hydrophobic core linker did not seem to play an effective role though a hydrophobic end group usually decreases the T_c.[10] The bigger the hydrophobic core, the lower T_c of a *s*-PDMAEMA should occur. Nevertheless, just the opposite, the *s*-PDMAEMA$_3$ displayed a lowest T_c while *s*-PDMAEMA$_{12}$ had the highest. For the different types of *s*-PDMAEMAs possessing a high identical DP (600 and 1200), the T_c did not exhibit any regular changes when the arm number was varied (Figure 5). The reason for this phenomenon is still unclear and seems to be quite complicated. Further investigations in this area are needed.

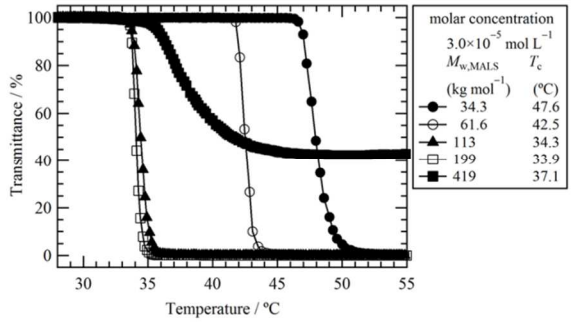

Figure 4. Optical transmittance dependence of *s*-PDMAEMA$_{12}$ on molecular weight at the fixed molar concentration of 3.0×10^{-5} mol L^{-1}

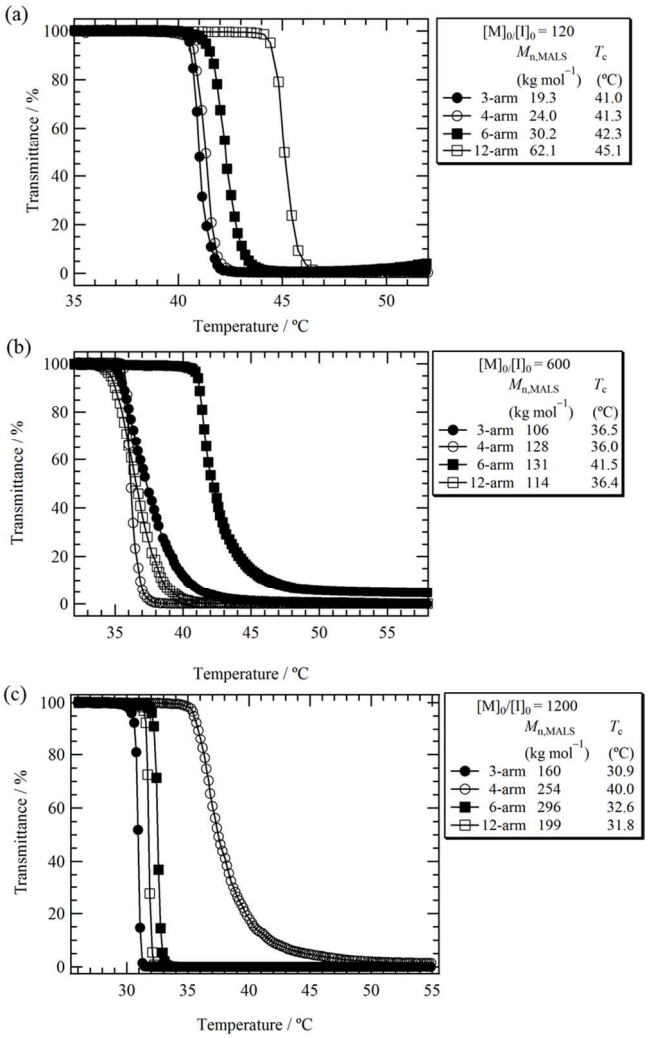

Figure 5. Arm-number dependence of cloud point for star-shaped PDMAEMAs, (a) [M]$_0$/[I]$_0$ = 120 (2.0 g L^{-1}), (b) [M]$_0$/[I]$_0$ = 600 (2.0 g L^{-1}), (c) [M]$_0$/[I]$_0$ = 1200 (10 g L^{-1}).

Table 2. Average hydrodynamic diameter of *s*-PDMAEMA$_{12}$s [a]

	run	[DMAEMA]$_0$/ [Initiator]$_0$	$M_{w,MALS}$ (kg mol^{-1})/($Đ$)	D_h (nm)		T_c (°C) [b]
				25 °C	55 °C	
s-PDMAEMA$_{12}$	17	120	34.3 (1.13)	5.7	306	45.1
	18	240	61.6 (1.22)	7.7	381	43.6
	19	600	114 (1.29)	9.4	160	36.5
	20	1200	199 (1.19)	11.3	56.1	38.5
	21	2400	419 (1.39)	16.0	27.5	41.4

[a] Determied by dynamic light scattering (DLS); solvent, deionized water; concentration, 2.0 g L^{-1}; scattering angle, 90°. [b] Determined by turbidimetry; conditions: solvent, deionized water; concentration, 2.0 g L^{-1}; heating rate, 1.0 °C min^{-1}; λ, 500 nm.

Conclusions

Three-, four-, six-, and twelve-armed star-shaped as well as linear PDMAEMAs with $M_{w,MALS}$ controlled in the range of 11.8 ~ 419 kg mol^{-1} and $Đ$ ≤1.39 were successfully synthesized by *t*-Bu-P$_4$-catalyzed GTP using multi-functional initiators which bear multiple silyl ketene acetal moieties. The arm uniformity and number of the resulting *s*-PDMAEMAs were evidenced by a cleavage experiment that involves retro-esterifying the core linker and esterifying back the hydrolyzed DMAEMA units. A MALDI-TOF MS measurement of the cleaved arm showed only one series of peaks, apparently suggesting that no side reactions occurred during the entire polymerization process though the arm number was up to twelve. It turns out that the thermoresponsive behavior of a *s*-PDMAEMA in terms of the responsive rate and T_c was significantly dependent on its concentration and $M_{w,MALS}$, but the dependence on the arm number at a similar $M_{w,MALS}$ was not very clear. In particular, the $M_{w,MALS}$ effect on the T_c was found to be quite different from those previous reports, in which the T_c of *l*-PDMAEMAs showed a monotonic decreasing tendency with the increase of molecular weight.[17] That is, the T_c of a *s*-PDMAEMA showed a decreasing trend with the increase of $M_{w,MALS}$ when its $M_{w,MALS}$ is less than a certain value around 100 kg mol^{-1}, while reversed to show an increasing trend after the $M_{w,MALS}$ is higher than this value. To the best of our knowledge, this is the first report to reveal such a special thermoresponsive phenomenon. The reason for such phenomenon can be roughly interpreted by a "cooperative hydration" model or the diffusion effect of a thermoresponsive polymer in solution. The fundamental study in this work is expected to provide information for designing branched thermoresponsive polymers. In addition, the synthesized *s*-PDMAEMAs are expected to have applications in ion depositor,[37] drug delivery system (DDS),[38,39] and so on. More investigations will be carried out in this area.

Acknowledgements

This work was financially supported by the MEXT (Japan) program "Strategic Molecular and Materials Chemistry through Innovative Coupling Reactions" of Hokkaido University and the MEXT Grant-in-Aid for Scientic Research on Innovative Areas "Advanced Molecular Transformation by Organocatalysts".

Notes and references

[a] *Graduate School of Chemical Sciences and Engineering, Hokkaido University, N13W8, Kita-ku, Sapporo 060-8628, Japan*
[b] *Faculty of Engineering, Hokkaido University, N13W8, Kita-ku, Sapporo 060-8628, Japan. E-mail: kakuchi@poly-bm.eng.hokudai.ac.jp*

† Electronic Supplementary Information (ESI) available: ^{1}H NMR, ^{13}C NMR, SEC, MALDI-TOF MS, and DLS data are available. See DOI: 10.1039/b000000x/

1 Ward, M. A.; Georgiou, T. K. *Polymers* 2011, **3**, 1215-1242.
2 Schmaljohann, D. *Adv. Drug Deliv. Rev.* 2006, **58**, 1655-1670.
3 Liu, R.; Fraylich, M.; Saunders, B. R. *Colloid Polym. Sci.* 2009, **287**, 627-643.
4 Scarpa, J. S.; Muller, D. D.; Klotz, I. M. *J. Am. Chem. Soc.* 1967, **89**, 6024-6030.
5 Seuring, J.; Agarwal, S. *Macromol. Rapid Commun.*, 2012, **33**, 1898-1920.
6 Roy, D.; Brooks, W. L. A.; Sumerlin, B. S. *Chem. Soc. Rev.*, 2013, **42**, 7214-7243.
7 Aseyev, V.; Tenhu, H.; Winnik, F. M. *Adv. Polym. Sci.*, 2010, **242**, 29-89.
8 Liu, H. Y.; Zhu, X. X. *Polymer* 1999, **40**, 6985-6990.
9 Qiu, X. P.; Koga, T.; Tanaka, F.; Winnik, F. M. *Sci. China Chem.* 2013, **56**, 56-64.
10 Narumi, A.; Fuchise, K.; Kakuchi, R.; Toda, A.; Satoh, T.; Kawaguchi, S.; Sugiyama, K.; Hirao, A.; Kakuchi, T. *Macromol. Rapid Commun.* 2008, **29**, 1126-1133.
11 Schild, H. G.; Terrell, D. A. *J. Phys. Chem.* 1990, **94**, 4352-4356.
12 Xia, Y.; Burke, A. D.; Stöver, H. D. H. *Macromolecules* 2006, **39**, 2275-2283.
13 Iha, R. K.; Wooley, K. L.; Nyström, A. M.; Burke, D. J.; Kade, M. J.; Hawker, C. J. *Chem. Rev.* 2009, **109**, 5620–5686.
14 Lutz, J.-F.; Hoth, A. *Macromolecules* 2006, **39**, 893-896.
15 Han, S.; Hagiwara, M.; Ishizone, T. *Macromolecules* 2003, **26**, 8312-8319.
16 Lutz, J.-F.; Akdemir, Ö.; Hoth, A. *J. Am. Chem. Soc.* 2006, **128**, 13046-13047.

17 Bütün, V.; Armes, S. P.; Billingham, N. C. *Polymer* 2001, **42**, 5993-6008.
18 Plamper, F. A.; Ruppel, M.; Schmalz, A.; Borisov, O.; Ballauff, M.; Müller, A. H. E. *Macromolecules* 2007, **40**, 8361-8366.
19 Plummer, R.; Hill, D. J. T.; Whittaker, A. W. *Macromolecules*, 2006, **39**, 8379-8388.
20 Xu, J.; Liu, S. *J. Polym. Sci., Part A: Polym. Chem.* 2009, **47**, 404-419.
21 Schmalz, A.; Hanisch, M.; Schmalz, Müller, A. H. E. *Polymer* 2010, **51**, 1213-1217.
22 Plamper, F. A.; Schmalz, A.; Chang, E. P.; Drechsler, M.; Jusufi, A.; Ballauff, M.; Müller, A. H. E. *Macromolecules* 2007, **40**, 5689-5697.
23 Hadjichristidis, N.; Iatrou, H.; Pitsikalis, M.; Mays, J. *Prog. Polym. Sci.* 2006, **31**, 1068-1132.
24 Aoshima, S.; Kanaoka, S. *Adv. Polym. Sci.*, 2010, **210**, 169-208.
25 Chen, Y.; Fuchise, K.; Narumi, A.; Kawaguchi, S.; Satoh, T.; Kakuchi, T. *Macromolecules* 2011, **44**, 9091-9098.
26 Chen, Y.; Takada, K.; Fuchise, K.; Satoh, T.; Kakuchi, T. *J. Polym. Sci., Part A: Polym. Chem.* 2012, **50**, 3277-3285.
27 Raynaud, J.; Liu, N.; Gnanou, Y.; Taton, D. *Macromolecules* 2010, **43**, 8853-8861.
28 Tsuboi, Y.; Tada, T.; Shoji, T.; Kitamura, N. *Macromol. Chem. Phys.* 2012, **213**, 1879-1884.
29 Tsuboi, Y.; Kikuchi, K.; Kitamura, N.; Shimomoto, H.; Kanaoka, S.; Aoshima, S. *Macromol. Chem. Phys.* 2012, **213**, 374-381.
30 Zhen, Q.; Pan, C.-Y. *Eur. Polym. J.* 2006, **42**, 807-814.
31Georgiou, T. K.; Vamvakaki, M.; Patrickios, C. S. *Biomacromolecules* 2004, **5**, 2221-2229.
32 Okada, Y.; Tanaka, F. *Macromolecules* 2005, **38**, 4465-4471.
33 Luo, S.; Xu, J.; Zhu, Z.; Wu, C.; Liu, S. *J. Phys. Chem. B* 2006, **110**, 9132-9139.
34 Xu, J.; Luo, S.; Shi, W.; Liu, S. *Langmuir* 2006, **22**, 989-997.
35 Patterson, D. *Macromolecules* 1969, **2**, 672-677.
36 Xia, Y.; Bruke, A. D.; Stöver, H. D. H. *Macromolecules* 2006, **39**, 2275-2283.
37 Yang, J.; Cao, S.; Xin, J.; Chen, X.; Wu, W.; Li, J. *J. Polym. Res.* 2013, **20**, 157-166.
38 Chen, X.; Wu, W.; Guo, Z.; Li, J. *Biomaterials.* 2011, **32**, 1759-1766.
39 Wu, W.; Liu, J.; Cao, S.; Tan, H.; Li, J.; Xu, F.; Zhang, X. *Int. J. Pharm.* 2011, **416**, 104-109.

For Table of Contents Graphical Abstract Use Only

Thermoresponsive Properties of 3-, 4-, 6-, and 12-Armed Star-Shaped Poly[2-(dimethylamino)ethyl methacrylate]s Prepared by Core-First Group Transfer Polymerization

Seiya Kikuchi,[a] Yougen Chen,[b] Keita Fuchise,[b] Kenji Takada,[a] Junsuke Kitakado,[a] Shin-ichiro Sato,[b] Toshifumi Satoh,[b] and Toyoji Kakuchi*[b]

The thermoresponsive behavior of 3-, 4-, 6-, and 12-armed star-shaped poly[2-(dimethylamino)ethyl methacrylate]s prepared by group transfer polymerization was intensively investigated, based on the evaluation of the respective effect of mass concentration in aqueous solution, molecular weight, or arm number of the resulting polymers on their cloud points.

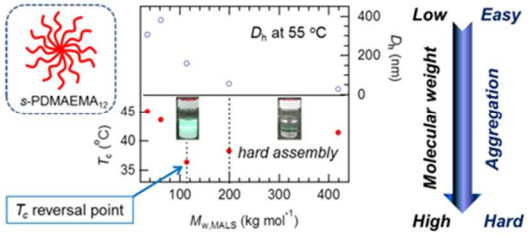

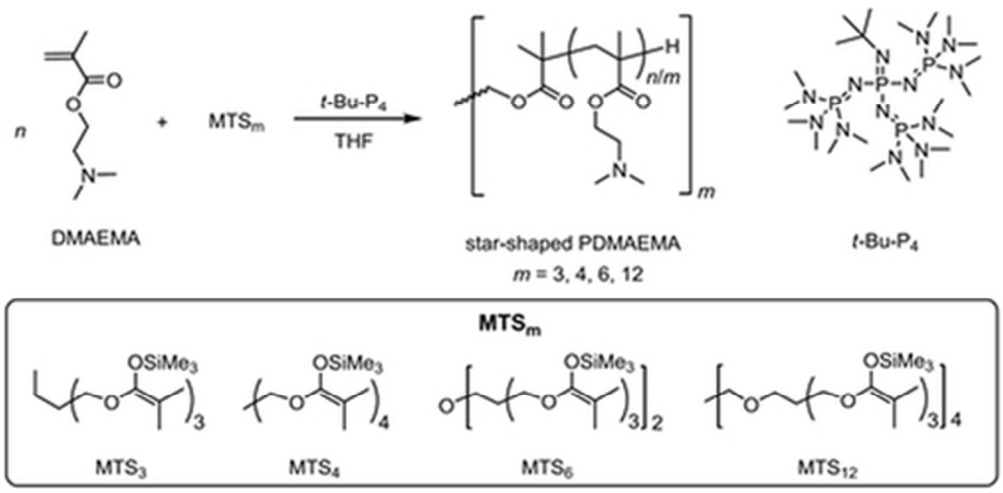

42x20mm (300 x 300 DPI)

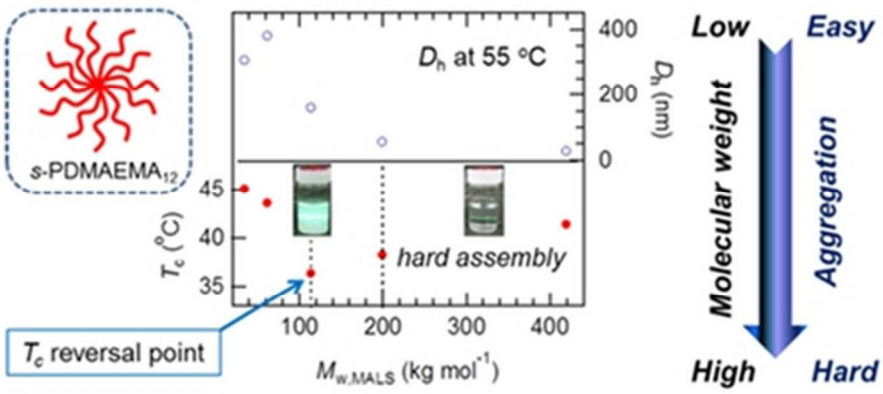

37x17mm (300 x 300 DPI)